

MICROWAVE AND MILLIMETER WAVE TESTING FOR THE INSPECTION OF THE SPACE SHUTTLE SPRAY ON FOAM INSULATION (SOFI) AND THE ACREAGE HEAT TILES

R. Zoughi¹, S. Kharkovsky¹, and F.L. Hepburn²

¹Applied Microwave Nondestructive Testing Laboratory (*amntl*)
Electrical and Computer Engineering Department
University of Missouri-Rolla, Rolla, MO 65409

²NASA Marshall Space Flight Center
MSFC, AL 35812

ABSTRACT- The utility of microwave and millimeter wave nondestructive testing and evaluation (NDT&E) methods, for testing the Space Shuttle's external fuel tank spray on foam insulation (SOFI) and the acreage heat tiles has been investigated during the past two years. Millimeter wave NDE techniques are capable of producing internal images of SOFI. This paper presents the results of testing several diverse panels with embedded voids and debonds at millimeter wave frequencies. Additionally, the results of testing a set of heat tiles are also presented. Finally, the attributes of these methods as well as the advantageous features associated with these systems are also provided.

Keywords: SOFI, heat tiles, millimeter waves

PACS:42.30.Va, 42.40.Jv, 84.40.-x

INTRODUCTION

It has been determined that the Space Shuttle Columbia's disaster was caused by a dislodged piece of spray on insulating foam (SOFI) from the external fuel tank that struck the leading edge of the left wing [1]. Since then several potential nondestructive testing (NDT) methods have been considered and their utility investigated for the inspection of the external tank SOFI including microwave and millimeter wave NDT methods [1-6]. During the past two years these methods have been expanded to encompass the higher end of the microwave frequency spectrum; namely, the millimeter wave frequency range. Microwave frequency range begins from about 300 MHz to 30 GHz at which point millimeter wave frequency range begins and ends at 300 GHz [7]. Millimeter wave frequency range corresponds to 10 mm – 1 mm range of wavelength. These are well-established and accepted standard frequency spectra for microwave and millimeter waves [7]. These frequencies ranges also encompass several standard waveguide bands such as Ka-band (26.5-40 GHz), V-band (50-75 GHz), W-band (75-110 GHz) and W-band (110-170 GHz) as it relates to this millimeter wave NDT of SOFI. The low permittivity and low loss (both attenuation and scattering (e.g., extinction) nature of SOFI makes this

method a great candidate for inspecting the SOFI for undesired anomalies such as voids and debonds.

In addition, the utility of microwave NDT has also been investigated for the inspecting of the Space Shuttle acreage heat tiles. These tiles are also in the family of low loss dielectric (ceramic) materials and microwave signals can easily penetrate inside of them and expose any undesired flaw (such as debonds) that may exist between the orbiter's fuselage and the tiles.

The success of the previous investigations in using these NDT methods led to a broader investigation involving the use of focused microwave and millimeter wave techniques. The term focusing in this context encompasses both real aperture and synthetic aperture focusing techniques. This paper presents the results of using millimeter wave NDT for imaging several specially-prepared SOFI panels with embedded flaws (voids and debonds). The results of using microwave and millimeter wave NDT methods for inspecting a set of heat tile panels are also provided. The positive attributes of microwave and millimeter wave NDT methods have been outlined elsewhere and will not be repeated here [3-4, 8].

SOFI MILLIMETER WAVE IMAGING RESULTS

Millimeter wave reflectometers were designed and assembled for this purpose. Subsequently, using 2D automated scanning tables, raster scans (images) of several SOFI panels were produced. Additionally, in some cases images at two orthogonal polarizations; namely, parallel to and perpendicular to the stringer axes were produced. Polarization of the transmitted and received waves can be manipulated to enhance some images by reducing the influence of unwanted reflections from hard targets such as edges of stringers, flange, bolts, etc.

The first panel consisted of an 8"-thick piece of SOFI on an aluminum substrate with voids and debonds inserts located at the substrate. The voids were produced by hollowing out a cube of SOFI and the debonds were made out of thin pieces of SOFI cut and placed on the substrate. One of the voids had a diagonal cut across it, as shown in Fig. 1. These inserts were collectively arranged for evaluating the potential of method for detecting different sizes and shapes of anomalies. For more detail about this panel the reader is referred to reference [4]. Figure 2 shows the millimeter wave image of this panel at 100 GHz using a lens antenna with a footprint of 0.25" (in diameter). The results clearly show that all of the inserts are detected with their relative sizes and locations also clearly indicated. The presence of the diagonal is very vividly shown in this image as well. The large quarter circular features in the image are primary as a result of the fact that the panel substrate was bowed (i.e., its four corners were lifted up during the manufacturing of the panel) [4].

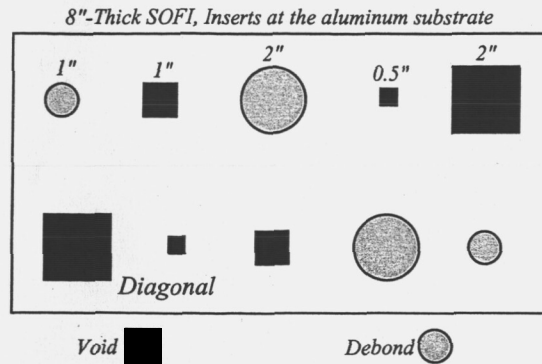


FIGURE 1. Schematic of the 8"-thick SOFI panel.

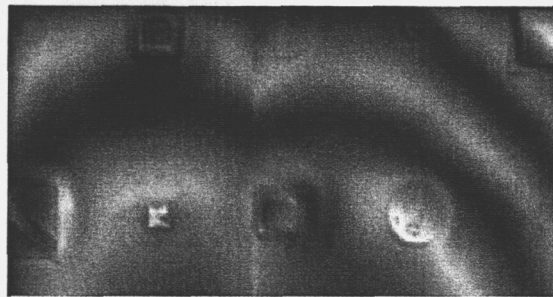
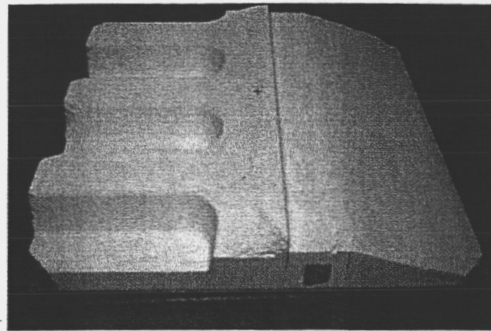
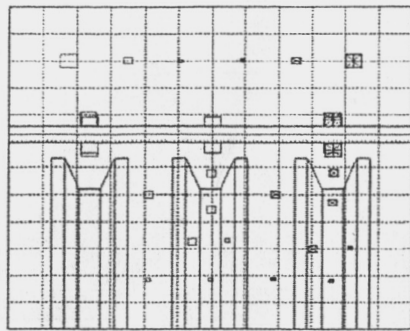


FIGURE 2. Image of the 8"-thick SOFI panel at 100 GHz.

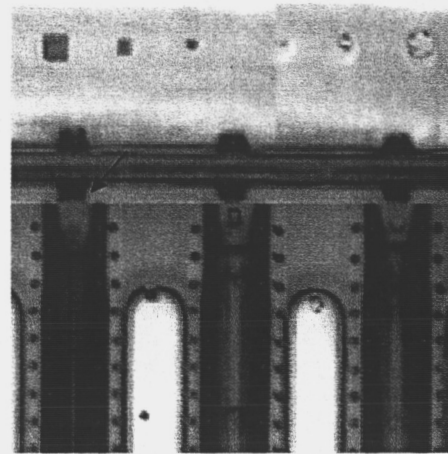
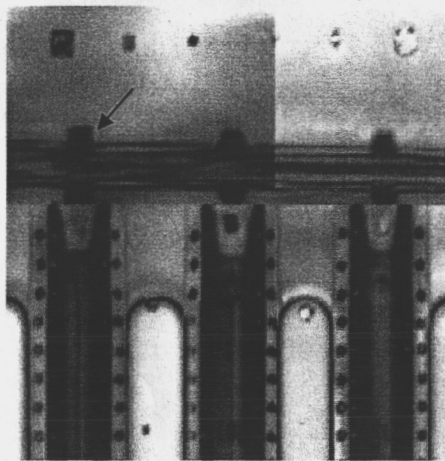
The next panel, referred to as the POD panel, was designed to closely represent a section of the external tank possessing a complex geometry. This panel had three stringers, a flange and three bolts and the SOFI was applied in the same manner and shape as what would be encountered in the external fuel tank. Additionally, several SOFI inserts representing voids and debonds as well as several rubber inserts were embedded in this panel. The rubber inserts were placed for comparative studies and are not expected to be found in the external tank. Figures 3a-b show the schematic and a picture of this panel. Figures 4a-b show the parallel and perpendicular polarization images of this panel at 100 GHz, respectively. For this image the lens antenna was focused at the panel substrate. From these images one can see that most of the inserts were detected with the exception of the inserts that were placed at the sides of the stringers and some of the inserts below the bolts. Figures 5a-b show a similar set of images but with the lens focused on top of the stringers. These results clearly show the rubber inserts on the sides of the middle stringer and an impression of the rubber insert below the left bolt. It is also evident that the parallel polarization results show the inserts on the sides of the stringer much better than the perpendicular polarization results. This fact was consistently experienced throughout this investigation. The primary reason for this is the fact that when the electric field is parallel to the stringer axes, the reflection at the edges of the stringer are less prominent than when using the perpendicular polarization. In this way fainter anomalies near the stringer edges are more likely detected using the parallel polarization.



(a)

(b)

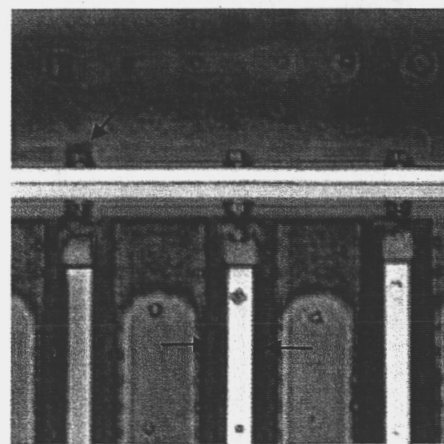
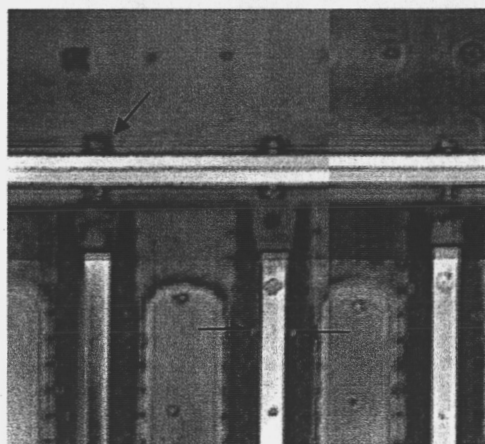
FIGURE 3. POD panel: (a) schematic and (b) picture.



(a)

(b)

FIGURE 4. 100 GHz image of the POD panel with lens focused on the aluminum substrate: (a) parallel polarization and (b) perpendicular polarization.



(a)

(b)

FIGURE 5. 100 GHz image of the POD panel with the lens focused on top of the stringers: (a) parallel polarization and (b) perpendicular polarization.

Another panel (POD 50R) with six stringers was also investigated. Figure 6 shows a picture of this panel. Several SOFI inserts representing voids and debonds were placed around two of the stringers in this panel. One SOFI insert was placed in one of the stringer opening regions and a small insert was placed under one of the bolts. This panel was also imaged at 100 GHz. Figure 7 shows the image of this panel with two smaller images highlighting the detected inserts. The insert underneath the bolt was not detected.

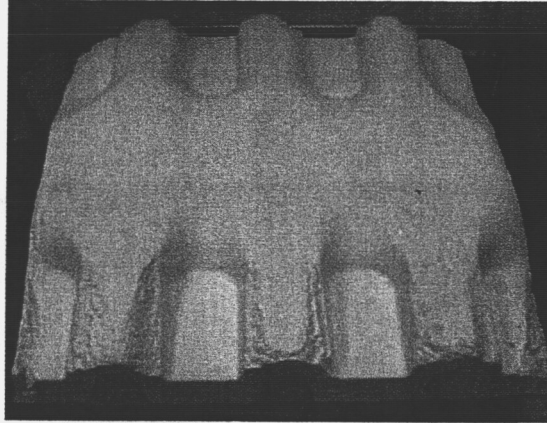


FIGURE 6. Picture of SOFI (POD 50R) panel.

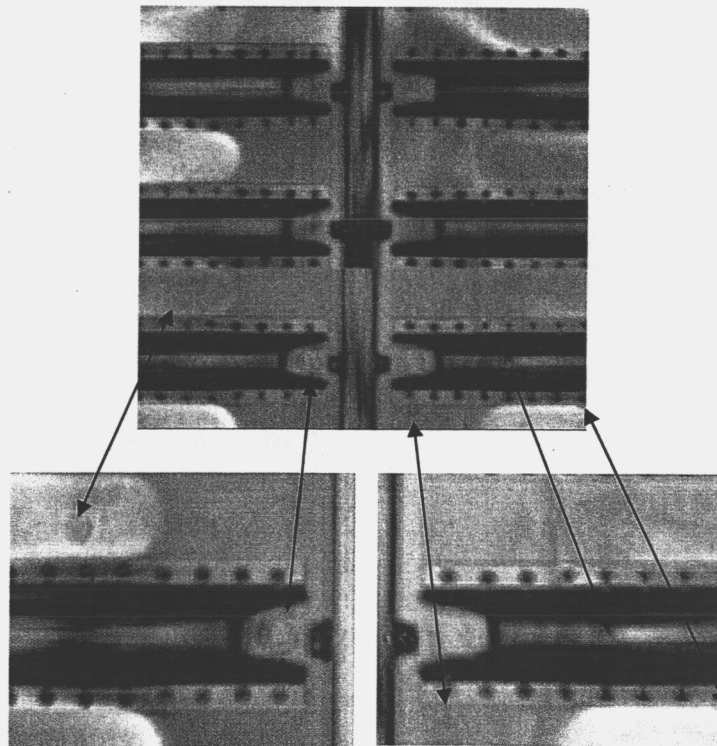


FIGURE 7. 100 GHz image of SOFI panel (POD 50R) with two sub-images highlighting the inserts.

ACREAGE HEAT TILE IMAGING RESULTS

Twelve heat tiles were assembled into a panel, as shown in Figure 8. The relative thickness of the tiles varied from one tile to another in addition to the fact that each individual heat tile had a non-uniform thickness, as shown in Figure 8. Several simulated defects were embedded in this panel which consisted of areas representing repaired regions and debonds. Moreover, a thin air pocket was created in the substrate under some of the tiles. Images of this panel were produced using reflectometers with small horn antenna radiators at Ka-band and V-band. Figure 9 shows three such images at 33.5 GHz, 67 GHz and 70 GHz, respectively (with the types of defects indicated by numbers). The results show that at 33.5 GHz (Fig. 9a) two repair regions, a debond and an air pocket are clearly detected. There is an indication of another repair region in the middle top square tile. However, this indication does not correspond to the defect map of this panel and may be the indication of an unintended manufacturing anomaly. One of the air pockets and debonds were also detected at this frequency.

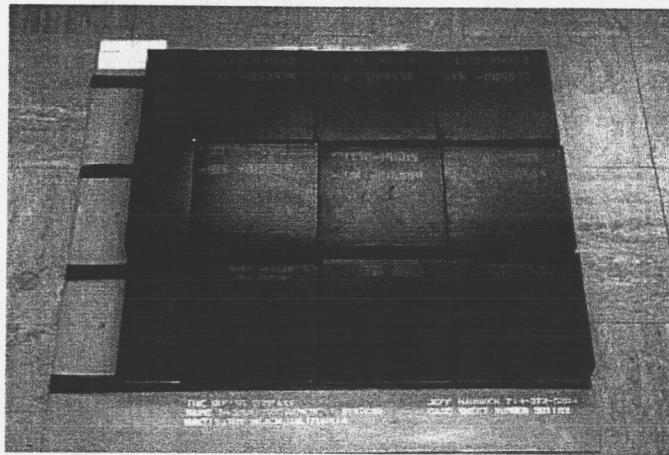


FIGURE 8. Picture of the heat tile panel consisting of twelve separate heat tiles.

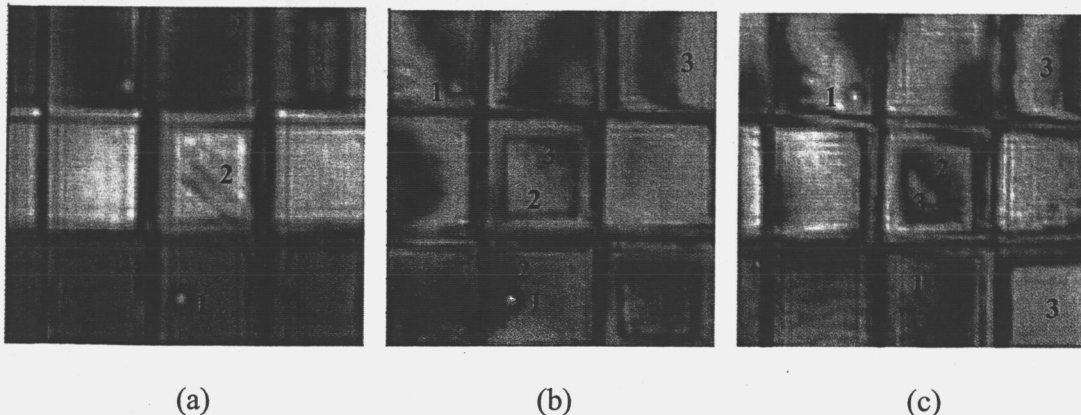


FIGURE 9. Images of the heat tile panel at: (a) 33.5 GHz (Ka-band), (b) 67 GHz (V-band) and (c) 70 GHz (V-band) - (1- repair region), (2- debond) and (3- air pocket in the substrate).

The results at 67 GHz show the presence of the two repair regions. Two of the larger air pockets along with a smaller one (top right corner tile) are detected as well. It is important to note that a detectable indication of a small debond near one of the repair regions (lower middle tile) is also seen in this image. The results at 70 GHz (Fig. 9c) are similar to those obtained at 67 GHz. Overall, the image at lower frequency (Ka-band) seemed to produce the best results. The air pockets were not detected well at this frequency, while they were better detected at V-band frequencies. However, there is less significant number of indications in the Ka-band image, compared to the V-band images, that could be interpreted as anomalies that do not really exist in the panel (i.e., false indications). Additional investigation of this acreage heat tile panel (not shown here) consistently showed higher microwave frequencies (K-band, 18-26.5 GHz) and lower millimeter wave frequencies (Ka-band, 26.5-40 GHz) to be more effective for imaging the acreage heat tiles. The image shown in Fig.9a (33.5 GHz) was not necessarily obtained using optimal measurement parameters. It is expected that a more detailed investigation of the acreage heat tiles at these frequencies will render most of the anomalies and structural features (i.e., air pockets) detectable (future investigation).

SUMMARY AND DISCUSSIONS

The results of this investigation has clearly shown the potential utility of using millimeter wave continuous wave (CW) imaging for testing different SOFI panels containing a diverse array of inserts simulating voids and debonds. Microwave and millimeter wave nondestructive testing techniques are quite mature [8]. Using these systems and employing low incident power (less than 10 mW) and focused lenses or small horn antennas it was shown that it is readily possible to inspect SOFI that is 10" thick (and more). It is important to note that SOFI is primarily a low loss and low permittivity polymer material. Therefore, the dielectric loss factor associated with the SOFI polymer is not a cause of great signal attenuation. However, the microstructure of the SOFI (i.e., the tiny air bubbles that makes it to be a foam) can cause considerable scattering at frequencies higher than ~250 GHz. Therefore, at much higher than millimeter wave range frequencies the extinction coefficient (which accounts for both attenuation and scattering) may be high and therefore signal penetration into SOFI may be limited. Through these investigations it was also found that the sensitivity to surface rind (where SOFI acreage areas) is minimal and therefore this surface feature is not a limiting factor is using these methods.

One of the most important attributes of these focused CW millimeter wave techniques is the fact that anomalies at different depths within the SOFI are detected. This is the results of the fact that although the lens may be focused at a certain depth in a SOFI panel (e.g., top of stringers), however, the depth of focus associated with a lens (usually a few inches depending on the frequency and the design of the lens) renders anomalies at other depths detectable. At depths, not coinciding with the lens focal length, the indication of these anomalies will be somewhat blurred but not totally missed. This is a significant advantage of these methods. Of course, once a blurred indication is detected, the lens distance to the SOFI may be changed to better focus it on the detected anomaly [4, 9].

No user facility modification is required when using these techniques since the necessary hardware that was used to produce the images shown here and (previously [3-4, 9]) are small, light weight, portable, easy-to-set up, robust, produce repeatable results and can be easily adapted to existing scanning platforms. In these investigations it was shown that embedded anomalies as thin as 0.125" at a depth of 8.25" were relatively easily detected. Future improvements may include using lenses with smaller footprints and systems operating at a slightly higher millimeter wave frequency.

ACKNOWLEDGMENT

This work was supported through a cooperative agreement from NASA George C. Marshall Space Flight Center, Huntsville, AL. The authors are also grateful to Mr. James L. Walker (NASA MSFC) for providing the panels and many insightful discussions..

REFERENCES

1. Columbia Accident Investigation Board Report, NASA, August 2003.
2. Shrestha S., S. Kharkovsky, R. Zoughi, F.L. Hepburn and G. Workman, "Microwave Nondestructive Inspection of Thick Insulating Foam," *The American Society for Non-Destructive Testing (ASNT) Fall Conference and Quality Testing Show*, Pittsburgh, PA, 13-17 October 2003.
3. Shrestha S., S. Kharkovsky, R. Zoughi and F.L. Hepburn, "Microwave and Millimeter Wave Nondestructive Evaluation of the External Tank Insulating Foam," *Materials Evaluation*, vol.63, no. 3, pp.339-344, March 2005.
4. Kharkovsky S., F. Hepburn, J. Walker and R. Zoughi. Nondestructive Testing of the Space Shuttle External Tank Foam Insulation using Near Field and Focused Millimeter Wave Techniques, *Materials Evaluation*, vol. 63, no. 5, pp. 516-522, May 2005.
5. Davis C., F. Santos, "Shearography NDE of Space Launch Vehicles," Presented at *The American Society for Non-Destructive Testing (ASNT) Fall Conference and Quality Testing Show*, Pittsburgh, PA, 13-17 October 2003.
6. Madaras E., "Terahertz NDE for Inspection of Shuttle Foam," Presented at *The American Society for Non-Destructive Testing (ASNT) Fall Conference and Quality Testing Show*, Pittsburgh, PA, 13-17 October 2003.
7. Pozar, D.M., *Microwave Engineering*, 2nd Edition, Addison Wesley Publishing Co., Inc., NY, 1990.
8. Zoughi, R., *Microwave Non-Destructive Testing and Evaluation*, Kluwer Academic Publishers, The Netherlands, 2000.
9. Kharkovsky S., J.T. Case, R. Zoughi and F. Hepburn. Millimeter Wave Detection of Localized Anomalies in the Space Shuttle External Fuel Tank Insulating Foam and Acreage Heat Tiles, *Proc. 22nd IEEE Instrumentation and Measurement Technology Conference*, Ottawa, Canada, pp.1527-1530, 2005.